High Performance Computing for Nanoplasmonic Laser Fusion

István Papp, Larissa Bravina, Mária Csete, Igor N. Mishustin, Dénes Molnár, Anton Motornenko, Leonid M. Satarov, Horst Stöcker, Daniel D. Strottman, András Szenes, Dávid Vass, Tamás S. Biró, László P. Csernai, Norbert Kroó

Nanoplasmonic Laser Fusion Research Laboratory

THEORETICAL GROUP:

- Csete, Mária, csoportvezető (SZTE)
- Papp, István (Wigner FK)
- Tóth, Emese (SZTE)
- Vass, Dávid (SZTE)
- Fekete, Olivér (SZTE)
- Szenes, András (SZTE)

MATERIAL PREPARATION GROUP:

- Bonyár, Attila, csoportvezető (BME ETT)
- Borók, Alexandra (BME ETT)
- Szalóki, Melinda (DE FOK)
- Petrik, Péter (EK)

LASER GROUP:

- Rácz, Péter, csoportvezető (Wigner FK)
- Dombi, Péter (Wigner FK)
- Kedves, Miklós (Wigner FK)
- Aladi, Márk (Wigner FK)

SPECTROSCOPY GROUP:

- Veres, Miklós, csoportvezető (Wigner FK)
- Rigó, István (Wigner FK)
- Nagyné Szokol, Ágnes (Wigner FK)
- Holomb, Román (Wigner FK)

Thermo-nuclear Fusion

- Fusion does not happen spontaneously on Earth
- Total fusion energy $E_f = \frac{1}{4}n^2\tau\epsilon\langle v\sigma\rangle$
- ηE_f is the usable energy
- The loss is $(1-\eta)(E_0 + E_b)$
- $E_0 = 3nkT$, $E_b = bn^2\tau\sqrt{T}$ (thermal bremsstralung)
- Giving the gain factor: $Q = \frac{\eta\epsilon n\tau v\sigma}{4(1-\eta)(3kT+bn\tau\sqrt{T})}$
- Q must be $Q > 1$ for energy production
- This also means $n\tau > \frac{3kT(1-\eta)}{\frac{1}{4}\epsilon\eta\langle v\sigma\rangle - b(1-\eta)\sqrt{T}} \rightarrow$ LC
- Fulfilling the Lawson criterion
    - Magnetically confined plasmas: increase confinement time
    - Inertial confinement fusion: increase density of fusion plasma

Direct vs Indirect drive

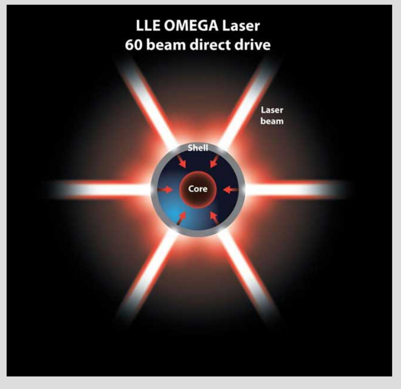

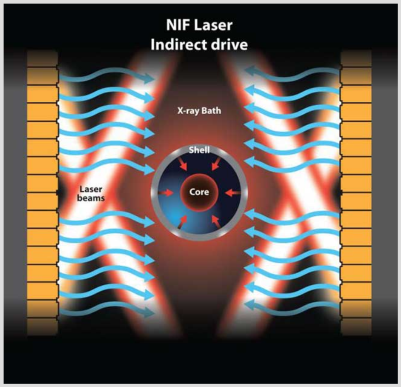

Hohlraum 2014

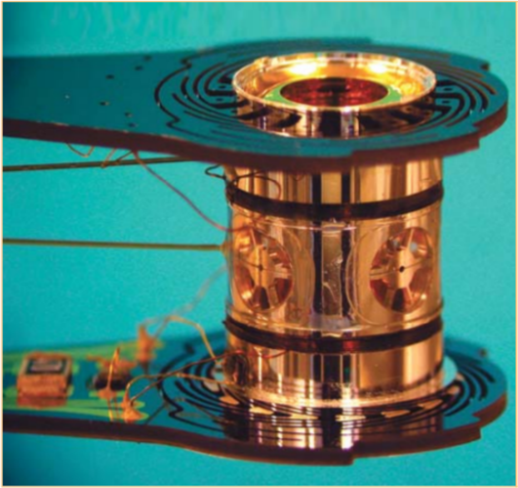

LAWRENCE LIVERMORE NATIONAL LABORATORY

A hohlraum made from gold and 1 cm tall contains the fusion fuel capsule used in experiments at the National Ignition Facility. Light from the laser enters the ends of the cylinder and is converted to x rays, which implode the capsule.

Hohlraum 2014

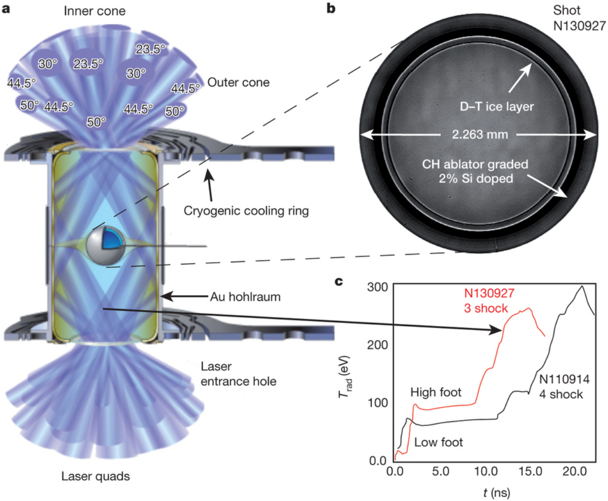

[O.A. Hurricane et al., Nature, 506, 343 (2014)]

Laser-Induced

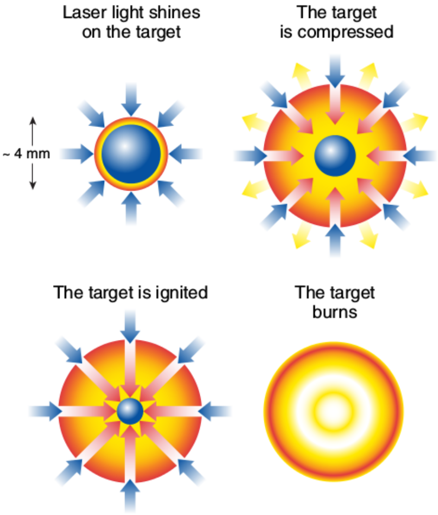

Rayleigh-Taylor instabilities

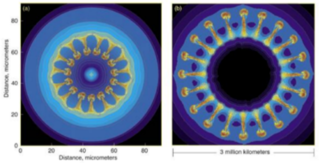

Striking similarities exist between hydrodynamic instabilities in (a) inertial confinement fusion capsule implosions and (b) core-collapse supernova explosions. [Image (a) is from Sakagami and Nishihara, *Physics of Fluids B* **2**, 2715 (1990); image (b) is from Hachisu et al., *Astrophysical Journal* **368**, L27 (1991).]

Energy must be delivered as sysmmetric as possible!

Different levels of corrugation of the shell surfaces :

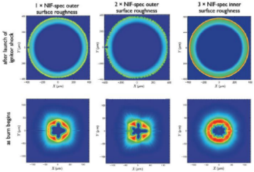

Left: same roughness of inner and outer surface as specified for the NIF target
Center: outer surface roughness is twice the NIF level
Right: DT inner surface roughness three times larger than NIF specifications

[S. Atzeni et al., Nucl. Fusion 54, 054008 (2014).]

25

RFD

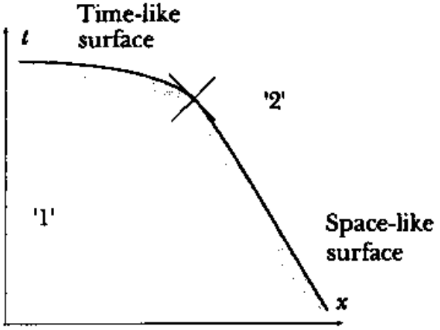

Figure 5.10: Smooth change from spacelike to timelike detonation

[Csernai, L.P. (1987). Detonation on a time-like front for relativistic systems. Zh. Eksp. Teor. Fiz. 92, 379-386.]

Constant absorptivity

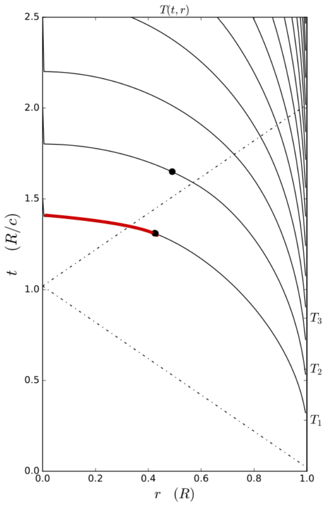

[L.P. Csernai & D.D. Strottman, Laser and Particle Beams 33, 279 (2015)]

$$\alpha_{k_{middle}} = \alpha_{k_{edge}}$$

Simultaneous volume ignition is only up to 12%

Doping with gold

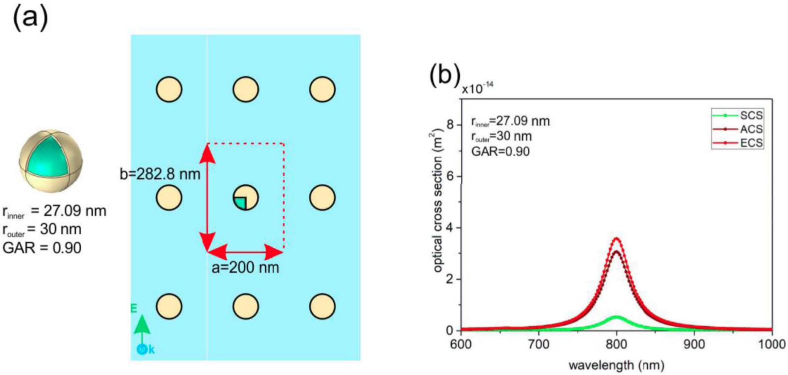

(a) Left: Single core-shell nano-sphere. Right: Rectangular lattice of nano-spheres in a transverse layer of the target.
(b) Optical cross-section of an individual core-shell nano-sphere optimized to absorb light at 800 nm wavelength and optical response of the same core-shell nano-spheres composing a rectangular lattice.

Changing absorptivity

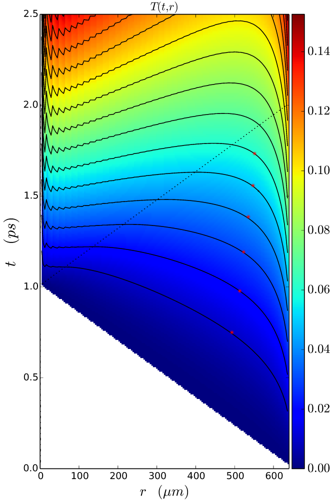

[Csernai, L.P., Kroo, N. and Papp, I. (2017). Procedure to improve the stability and efficiency of laser-fusion by nano-plasmonics method. Patent P1700278/3 of the Hungarian Intellectual Property Office.]

$\alpha_{k_{middle}} \approx 4 \times \alpha_{k_{edge}}$

Simultaneous volume ignition is up to 73%

Flat target

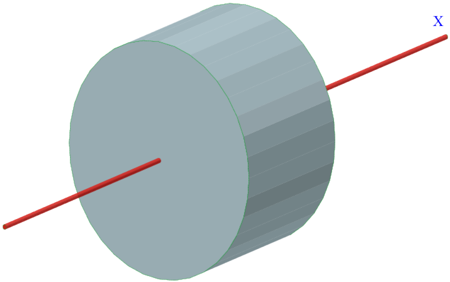

Schematic view of the cylindrical, flat target of radius, R, and thickness, h.
$V = 2\pi R^3, \quad R = \sqrt[3]{V/(2\pi)}, \quad h = \sqrt[3]{4V/\pi}.$

[L.P. Csernai, M. Csete, I.N. Mishustin, A. Motornenko, I. Papp, L.M. Satarov, H. Stcker & N. Kroó, Radiation- Dominated Implosion with Flat Target, *Physics and Wave Phenomena*, **28** (3) 187-199 (2020)]

Varying absorptivity

(a)

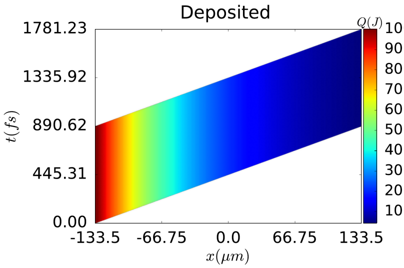

(b)

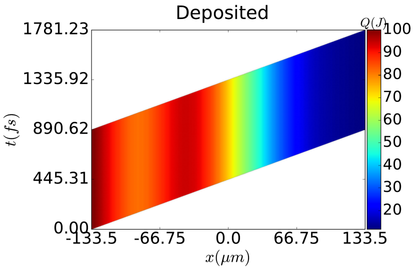

Deposited energy per unit time in the space-time plane across the depth, *h*, of the flat target. **(a) without** nano-shells **(b) with** nano-shells
To increase central absorption we used the following distribution:

$$\alpha_{ns}(s) = \alpha_{ns}^{C} + \alpha_{ns}(0) \cdot \exp\left[4 \times \frac{\left(\frac{s}{100}\right)^2}{\left(\frac{s}{100} - 1\right)\left(\frac{s}{100} + 1\right)}\right].$$

Similar configurations

Nuclear probes of an out-of-equilibrium plasma at the highest compression **Phys. Lett. A 383 (2019) 2285-2289.**

G. Zhang [a,b,*], M. Huang [c], A. Bonasera [d,e,*], Y.G. Ma [f,b,i,*], B.F. Shen [g,h,*], H.W. Wang [a,b], W.P. Wang [g], J.C. Xu [g], G.T. Fan [a,b], H.J. Fu [b], H. Xue [b], H. Zheng [j], L.X. Liu [a,b], S. Zhang [c], W.J. Li [b], X.G. Cao [a,b], X.G. Deng [b], X.Y. Li [b], Y.C. Liu [b], Y. Yu [g], Y. Zhang [b], C.B. Fu [k], X.P. Zhang [k]

4 (up) + 4(down) lasers
Target thickness, h (3.6μm-1mm) & radius, R, (150-400μm) were varied.

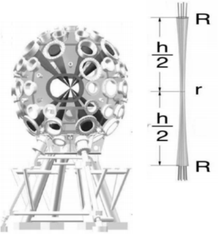

Total pulse energy 1.2kJ (2ns) for 8 beams.
Shortest (250ps) pulses -> 100s MeV ions > non-thermal distr. = directed ion acceleration

Typical fusion neutron energies were measured & used to extract the target density.

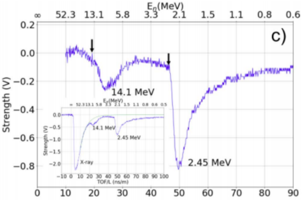

33

Similar configurations

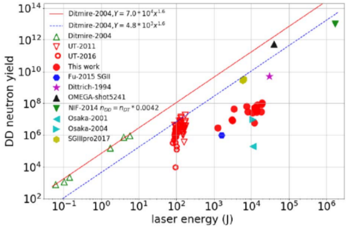

Figure 3: (color online) Fusion yield as function of laser energy. Different experimental results Ditmire-2004[40], UT-2011[20], UT-2016[19], Fu-2015 SGII[45], Dittrich-1994[49] , NIF-2014[48] , Osaka -2001[46], Osaka-2004[47], OMEGA-shot5241[41]and SGIIIpro2017[42] are indicated in the inset.

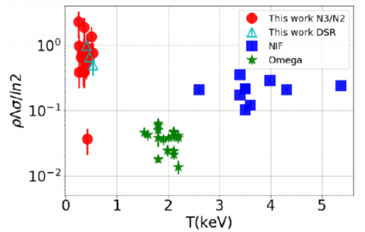

Figure 4: (color online) $\Lambda\rho\sigma/\ln 2$ obtained from eq.(4) vs T from eq.(1). Omega and NIF data are derived from the experiments[25], using the Down Scatter Ratio[23, 21]. Our results using the DSR method (N_4/N_3) are given by the open triangle symbols in good agreement with the N_3/N_2 ratios.

Experiment and collaboration

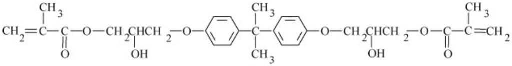

Bis-GMA

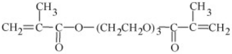

TEGDMA

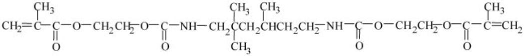

UDMA

Available software

Computational application	Web site	License	Availability	Canonical Reference
SHARP	[17]	Proprietary		doi:10.3847/1538-4357/aa6d13
ALaDyn	[18]	GPLv3+	Open Repo:[19]	doi:10.5281/zenodo.49553
EPOCH	[20]	GPL	Open to academic users but signup required :[21]	doi:10.1088/0741-3335/57/11/113001
FBPIC	[22]	3-Clause-BSD-LBNL	Open Repo:[23]	doi:10.1016/j.cpc.2016.02.007
LSP	[24]	Proprietary	Available from ATK	doi:10.1016/S0168-9002(01)00024-9
MAGIC	[25]	Proprietary	Available from ATK	doi:10.1016/0010-4655(95)00010-D
OSIRIS	[26]	Proprietary	Closed (Collaborators with MoU)	doi:10.1007/3-540-47789-6_36
PICCANTE	[27]	GPLv3+	Open Repo:[28]	doi:10.5281/zenodo.48703
PICLas	[29]	Proprietary	Available from Institute of Space Systems and Institute of Aerodynamics and Gas Dynamics at the University of Stuttgart	doi:10.1016/j.crme.2014.07.005
PIConGPU	[30]	GPLv3+	Open Repo:[31]	doi:10.1145/2503210.2504564
SMILEI	[32]	CeCILL-B	Open Repo:[33]	doi:10.1016/j.cpc.2017.09.024
iPIC3D	[34]	Apache License 2.0	Open Repo:[35]	doi:10.1016/j.matcom.2009.08.038
The Virtual Laser Plasma Library	[36]	Proprietary	Unknown	doi:10.1017/S0022377899007515
VizGrain	[37]	Proprietary	Commercially available from Esgee Technologies Inc.	
VPIC	[38]	3-Clause-BSD	Open Repo:[39]	doi:10.1063/1.2840133
VSim (Vorpal)	[40]	Proprietary	Available from Tech-X Corporation	doi:10.1016/j.jcp.2003.11.004
Warp	[41]	3-Clause-BSD-LBNL	Open Repo:[42]	doi:10.1063/1.860024
WarpX	[43]	3-Clause-BSD-LBNL	Open Repo:[44]	doi:10.1016/j.nima.2018.01.035
ZPIC	[45]	AGPLv3+	Open Repo:[46]	

Particle In Cell methods

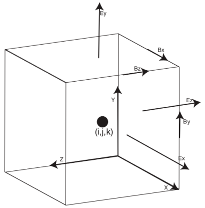

Figure 1. Yee staggered grid used for the Maxwell solver in *EPOCH*.

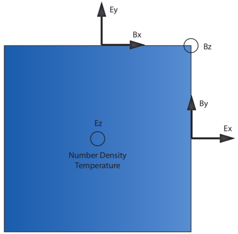

Figure 2: The Yee grid in 2D

[T.D. Arber et al 2015 Plasma Phys. Control. Fusion 57 113001]

A **super-particle** (**marker-particle**) is a computational particle that represents many real particles.

Particle **mover** or **pusher** algorithm as standard **Boris algorithm**.

Finite-difference time-domain method for solving the time evolution of **Maxwell's equations**.

General layout of the EPOCH code

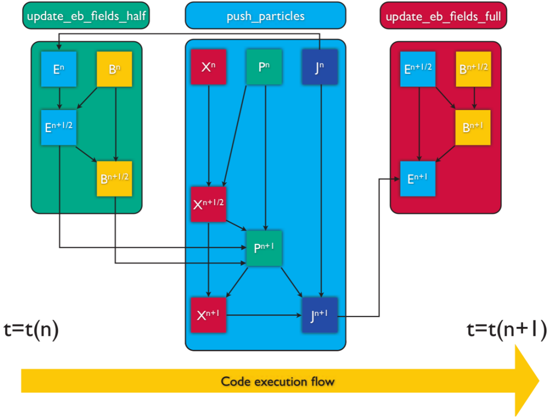

[EPOCH 4.0 dev manual]

- (input) deck
- housekeeping
- io
- parser
- physics_packages
- user_interaction

FDTD in EPOCH

- $\boldsymbol{E}_{n+\frac{1}{2}} = \boldsymbol{E}_n + \frac{\Delta t}{2}\left(c^2\nabla \times \boldsymbol{B}_n - \frac{\boldsymbol{j}_n}{\epsilon_0}\right)$
- $\boldsymbol{B}_{n+\frac{1}{2}} = \boldsymbol{B}_n - \frac{\Delta t}{2}\left(\nabla \times \boldsymbol{E}_{n+\frac{1}{2}}\right)$
- Call particle pusher which calculates j_{n+1}
- $\boldsymbol{B}_{n+1} = \boldsymbol{B}_{n+\frac{1}{2}} - \frac{\Delta t}{2}\left(\nabla \times \boldsymbol{E}_{n+\frac{1}{2}}\right)$
- $\boldsymbol{E}_{n+1} = \boldsymbol{E}_{n+\frac{1}{2}} + \frac{\Delta t}{2}\left(c^2\nabla \times \boldsymbol{B}_{n+1} - \frac{\boldsymbol{j}_{n+1}}{\epsilon_0}\right)$

Particle pusher

- Solves the relativistic equation of motion under the Lorentz force for each marker-particle

$$\boldsymbol{p}_{n+1} = \boldsymbol{p}_n + q\Delta t \left[\boldsymbol{E}_{n+\frac{1}{2}} \left(\boldsymbol{x}_{n+\frac{1}{2}} \right) + \boldsymbol{v}_{n+\frac{1}{2}} \times \boldsymbol{B}_{n+\frac{1}{2}} \left(\boldsymbol{x}_{n+\frac{1}{2}} \right) \right]$$

  $\boldsymbol{p}$ is the particle momentum q is the particle's charge $\boldsymbol{v}$ is the velocity.
  $\boldsymbol{p} = \gamma m \boldsymbol{v}$, where m is the rest mass $\gamma = \left[(\boldsymbol{p}/mc)^2 + 1 \right]^{1/2}$
- Villasenor and Buneman current deposition scheme [Villasenor J & Buneman O 1992 Comput. Phys. Commun. 69 306], always satisfied: $\nabla \cdot \boldsymbol{E} = \rho/\epsilon_0$, where ρ is the charge density.

Particle shape

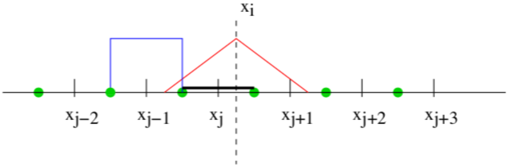

Figure 3: Second order particle shape function

First order approximations are considered

$$F_{part} = \frac{1}{2}F_{i-1}\left(\frac{1}{2}+\frac{x_i - X}{\Delta x}\right)^2 + \frac{1}{2}F_i\left(\frac{3}{4}-\frac{(x_i - X)^2}{\Delta x^2}\right)^2 + \frac{1}{2}F_{i+1}\left(\frac{1}{2}+\frac{x_i - X}{\Delta x}\right)^2$$

[EPOCH 4.0 dev manual]

A spicy code

Still beta version Supports:

- rough_box features
- grating
- grid stretching
- highly optimized output

1. A. Sgattoni, et. al., Laser-Driven Rayleigh-Taylor Instability: Plasmonics Effects and Three-Dimensional Structures, Phys. Rev. E, 91, 013106 (2015)
2. A. Sgattoni,et. al., High Energy Gain in Three-Dimensional Simulations of Light Sail Acceleration, Appl. Phys. Lett., 105, 084105 (2014)
3. L. Fedeli, et. al., Electron acceleration by relativistic surface plasmons in laser-grating interaction, Physical Review Letters 116, 015001 (2016)
4. A. Sgattoni, et. al., High field plasmonics and laser-plasma acceleration in solid targets, Plasma Physics and Controlled Fusion 58, 014004 (2015)

Benefits of a spicy code

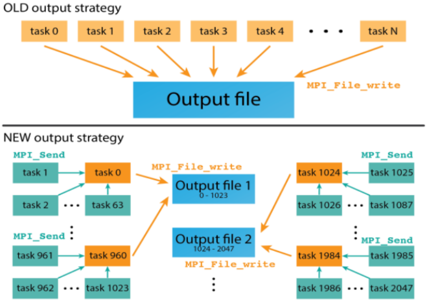

(a)

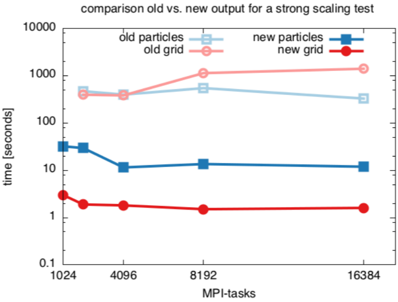

(b)

(a) Old and new strategies. G = 64 group of tasks and F = N/128 master tasks.
(b) Time spent for **writing particle positions** red, time spent for **grid based outputs** (EM fields, densities) marked with blue.

Ionisation

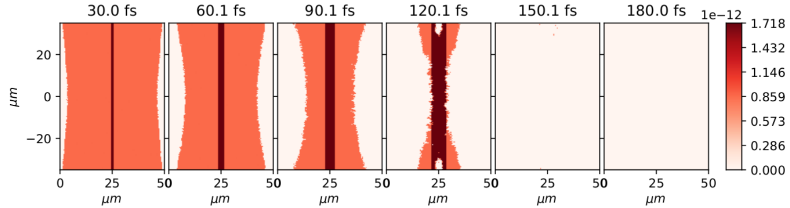

Figure 2: (color online) The ionization of the H atoms in a Laser Wake Field (LWF) wave due to the irradiation from both the $\pm x$- directions, on an initial target density of $n_H = 2.13 \cdot 10^{27}$ atoms/m^3 = $2.13 \cdot 10^{21}$ atoms/cm^3. The energy of the H atoms in Joule [J] per marker particle is shown. The H atoms disappear as protons and electrons are created. Due to the initial momentum of the colliding H slabs, the target and projectile slabs interpenetrate each other and this leads to double energy density. Several time-steps are shown at 30 fs time difference.

However **PICCANTE** does **not** contain ionisation
EPOCH includes a number of ionisation models by which electrons ionise in both the field of an intense laser and through collisions.
[Keldysh L 1965 Sov. Phys.JETP 20 1307]

Conclusions, Looking forward

- Mechanical, pressure driven processes are subject to RT instability, while shorter and more energetic irradiation can prevent the possibility of all mechanical instabilities.
- For more realistic estimates relativistic analysis is needed
- First steps include only smaller lasers with monomer targets
- PICCANTE unfinished, but with essential advantages
- For experimental physicists EPOCH is more user friendly